



Black carbon (BC) in a northern Tibetan mountain: effect of Kuwait fires on glaciers

Jiamao Zhou^{1,2}, Xuexi Tie^{1,3}, Baiqing Xu⁴, Shuyu Zhao¹, Mo Wang⁴, Guohui Li¹, Ting Zhang¹, Zhuizi Zhao^{1,5}, Suixin Liu¹, Song Yang⁴, Luyu Chang^{6,7}, and Junji Cao¹

¹KLACP, SKLLQG, Institute of Earth Environment, Chinese Academy of Sciences, Xi'an 710061, China

²University of Chinese Academy of Sciences, Beijing 100049, China

³Center for Excellence in Urban Atmospheric Environment, Institute of Urban Environment, Chinese Academy of Sciences, Xiamen 361021, China

⁴Key Laboratory of Tibetan Environment Changes and Land Surface Processes, Institute of Tibetan Plateau Research, Chinese Academy of Sciences, Beijing 100101, China

⁵School of Chemistry & Environmental Engineering, Jiangsu University of Technology, Changzhou 213001, China

⁶Shanghai Meteorological Service, Shanghai 200030, China

⁷Shanghai Key Laboratory of Meteorology and Health, Shanghai 200030, China

Correspondence: Xuexi Tie (tiexx@ieecas.cn) and Baiqing Xu (baiqing@itpcas.ac.cn)

Received: 4 May 2018 – Discussion started: 14 May 2018

Revised: 23 August 2018 – Accepted: 7 September 2018 – Published: 27 September 2018

Abstract. The black carbon (BC) deposition on the ice core at Muztagh Ata Mountain, northern Tibetan Plateau, was analyzed. Two sets of measurements were used in this study, which included the air samplings of BC particles during 2004–2006 and the ice core drillings of BC deposition during 1986–1994. Two numerical models were used to analyze the measured data. A global chemical transportation model (MOZART-4) was used to analyze the BC transport from the source regions, and a radiative transfer model (SNICAR) was used to study the effect of BC on snow albedo. The results show that during 1991–1992, there was a strong spike in the BC deposition at Muztagh Ata, suggesting that there was an unusual emission in the upward region during this period. This high peak of BC deposition was investigated by using the global chemical transportation model (MOZART-4). The analysis indicated that the emissions from large Kuwait fires at the end of the first Gulf War in 1991 caused this high peak of the BC concentrations and deposition (about 3–4 times higher than other years) at Muztagh Ata Mountain, suggesting that the upward BC emissions had important impacts on this remote site located on the northern Tibetan Plateau. Thus, there is a need to quantitatively estimate the effect of surrounding emissions on the BC concentrations on the northern Tibetan Plateau. In this study, a sensitivity study

with four individual BC emission regions (Central Asia, Europe, the Persian Gulf, and South Asia) was conducted by using the MOZART-4 model. The result suggests that during the “normal period” (non-Kuwait fires), the largest effect was due to the Central Asia source (44 %) during the Indian monsoon period, while during the non-monsoon period, the largest effect was due to the South Asia source (34 %). The increase in radiative forcing increase (RFI) due to the deposition of BC on snow was estimated by using the radiative transfer model (SNICAR). The results show that under the fresh snow assumption, the estimated increase in RFI ranged from 0.2 to 2.5 W m⁻², while under the aged snow assumption, the estimated increase in RFI ranged from 0.9 to 5.7 W m⁻². During the Kuwait fires period, the RFI values increased about 2–5 times higher than in the “normal period”, suggesting a significant increase for the snow melting on the northern Tibetan Plateau due to this fire event. This result suggests that the variability of BC deposition at Muztagh Ata Mountain provides useful information to study the effect of the upward BC emissions on environmental and climate issues in the northern Tibetan Plateau. The radiative effect of BC deposition on the snow melting provides important information regarding the water resources in the region.

1 Introduction

Black carbon (BC) particles emitted from combustion are considered an important air pollutant, as they have a direct effect by absorbing and scattering solar radiation, and an indirect effect by the change in cloud microphysical processes (acting as ice nuclei) and the efficiency of precipitation (acting as cloud condensation nuclei) (Ramanathan et al., 2001). Albedo changes induced by a strongly light-absorbing component deposited on the surface of snow and ice are key parameters in governing the radiative forcing and accelerate melting (Holben et al., 1998; Hansen and Nazarenko, 2004). These important properties make BC a key topic related to climate change, but are not well understood due to the very different inhomogeneous spatial and temporal distributions of BC, especially in remote areas such as the Tibetan Plateau.

BC particles can be deposited and preserved in the ice by the process of post-deposition on the glaciers and ice sheets. Retrieved ice cores from remote mountain glaciers and ice sheets provide useful information of the historical BC aerosol emissions and synchronous meteorology conditions. Previous studies on records of carbonaceous aerosols show that the emissions of fossil fuel combustion from central Europe had a significant impact on the glaciers in the Swiss Alps (Lavanchy et al., 1999). Bisiaux et al. (2012) analyzed two ice cores drilled in Antarctica and found that the ice core records of BC deposition reflected the change in atmospheric BC emission, distribution and transport in the Southern Hemisphere. By using an ice core in Greenland, the BC emissions from industrial activities and forest fires are differentiated (McConnell et al., 2007). These studies indicate that BC records in history are an important and practicable method to investigate the regional aerosol transport and emission variations.

In this study, the ice core BC at Muztagh Ata, northern Tibetan Plateau, is analyzed. Identification of the source regions, which have an important impact on BC deposition at Muztagh Ata, is a very important scientific issue, because of its location. In particular, there was a strong spike in the BC deposition during 1992–1993 at Muztagh Ata (as shown in the following text), reflecting the unusual emission in the upward region from Muztagh Ata. This strong spike in the ice core BC was about 3–4 times higher than in other years, producing important effects on the climate and hydrological cycle. As a result, the sources of BC which affect the ice core BC in this location need to be carefully studied. Muztagh Ata is located to the east of Pamir and in the north of the Tibetan Plateau. The ice core data provide important information for atmospheric circulation and climate change in Asia (An et al., 2001). Moreover, the climate in Muztagh Ata is very sensitive to solar warming mechanisms because it has a large snow cover in the region, resulting in important impacts on the hydrological cycle of the continent by enhancing glacier melt.

The BC sources which contribute the BC deposition on the Tibetan Plateau have been previously studied. Their results show that BC deposited on glaciers of the Pamir Mountains was emitted from Europe, the Middle East and central Asia (Liu et al., 2008; Xu et al., 2009a; Wang et al., 2015b), whereas BC deposition on snow and ice over the Himalayas and the southeastern Tibetan Plateau was mainly affected by the western upward regions in winter. During the Indian summer monsoon season, they were mainly affected by the BC sources in the Indian region (Ming et al., 2008; Xu et al., 2009b; Kaspari et al., 2011; Wang et al., 2015a). However, at present, the effects of the transport pathways and individual contributions of BC sources to the Muztagh Ata region have not been carefully studied. Because the radiative forcing caused by BC in snow and ice between different regions is very different, depending upon the emitting intensities, ocean–land distributions, topography, regional atmospheric circulations, and other factors, detailed studies of the source contributions to the region as well as the climate effect are needed to carefully study this important region.

Both the ice core deposition measurements at Muztagh Ata and a global chemical model (MOZART-4; Model for Ozone and Related chemical Tracers, version 4) are used in this study. To better evaluate the model performance, the air samples of BC particles during 2004–2006 were also analyzed. The global chemical transport model (MOZART-4) was used to analyze the long-term trend in the early 90s of the observed BC deposition and to quantify the individual contribution of different BC sources to the deposition on the snow cover. The modeled temporal variations and magnitude of the BC concentrations in the atmosphere and snow were compared to observations. Finally, a radiative transfer model (SNICAR) was used to study the effect of BC on snow albedo, radiative forcing, and runoff changes induced by the BC deposition on the Muztagh Ata snow.

2 Methodologies

2.1 Sampling sites

Muztagh Ata Mountain is located on the northern side of the Tibetan Plateau. Both atmospheric sampling and ice core drilling BC were conducted at the Muztagh Ata site. The atmospheric sampling BC (38°17.30' N, 75°01.38' E) was conducted in the Cold and Arid Regions Environmental and Engineering Institute, Chinese Academy of Sciences, at 4500 m above sea level (a.s.l.). A 170.4 m ice core (9.5 cm in diameter) was drilled during the summer season in 2012 from Kuokuosele (KKSL) Glacier of Muztagh Ata (38°11' N, 75°11' E; 5700 m a.s.l.), which was conducted by the Institute of Tibetan Plateau Research, Chinese Academy of Sciences. Because the site is surrounded by several important BC source regions, this measurement site is suitable for investigating the effect of BC emissions on the northern part

of the Tibetan Plateau, which plays important roles in global climate and hydrology (see Fig. 1).

The average annual temperature at the peak of the mountain is approximately -20°C . Because the numerous high mountains block the warm and humid air currents from the Indian and Pacific oceans, the climate in this area is relatively dry. The averaged annual precipitation is less than 200 mm, which is mainly snow to form perennial glaciers. There are 128 modern glaciers and on average about 377 km^2 . The prevailing winds in this region are usually westerly jet streams. Previous studies suggested that there was a very small effect by local sources, and the aerosol pollution originated mainly from the west by mid- and long-range transport. During summer, the South Asia monsoon also had an important effect on the transport of BC particles from India (Liu et al., 2008; Wu et al., 2008; Zhao et al., 2011; Wang et al., 2015b).

2.2 Measurements

During the period from 5 December 2003 to 17 February 2006, 81 valid total suspended aerosol particles (TSPs) were obtained with custom-made samplers at flow rates of 16 L min^{-1} . The measurements were conducted under very difficult environmental conditions, because of its high mountain location. The sampler power was supplied by solar energy and a storage battery. Each sample was collected over one week and on 15 mm Whatman quartz microfibre filter (QM/A, Whatman LTD, Maidstone, UK), which was pre-combusted at 800°C for 3 h to remove the potential carbon disturbance. The sample was identified as valid when its sampling standard volume was greater than 30 m^3 . As a result, the valid sample numbers for spring, summer, autumn, and winter were 19, 21, 14, and 27, respectively.

For the ice core measurement, a 170.4 m ice core (9.5 cm in diameter) was drilled during the summer season in 2012 from Kuokuosele (KKSL) Glacier of Muztagh Ata ($38^{\circ}11'\text{ N}$, $75^{\circ}11'\text{ E}$; 5700 m a.s.l.), which is close to the BC air sampling site. A stainless steel scalpel that was pre-cleaned at -5°C in a class 100 laminar flow bench was used to remove the outer layer of the ice core to exclude the pollutants that might be mixed in during drilling, transport, and storage. The ice core dating and calculation of BC deposition fluxes were provided by the Institute of Tibetan Plateau Research, Chinese Academy of Sciences. The detailed method for the measurement of BC deposition is shown by Xu et al. (2009a).

2.3 Analytical methods

The elemental carbon (EC, which is a proxy for BC in this study) analyses for atmospheric filters (TSP samples) were carried out by using a Desert Research Institute (DRI) Model 2001 carbon analyzer (Atmoslytic Inc., Calabasas, CA, USA) with the IMPROVE (Interagency Monitoring of PROtected Visual Environments) thermal/optical reflectance

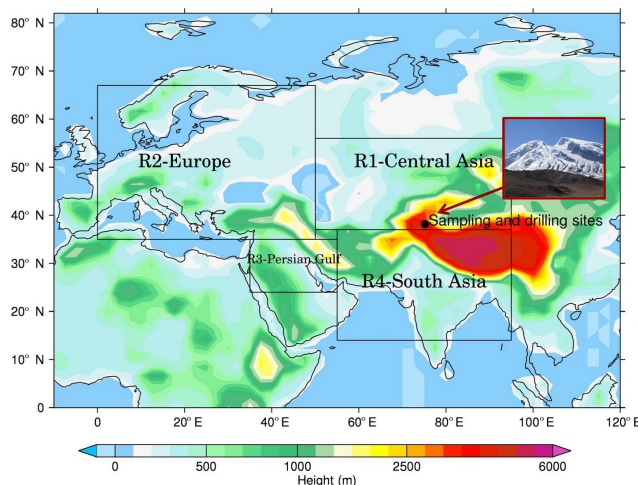


Figure 1. The Muztagh Ata measurement site (indicated by the dot), and the surrounding BC source areas (R1 – Central Asia region; R2 – European region; R3 – Persian Gulf region; and R4 – South Asia region).

(TOR) protocol (Chow et al., 1993, 2004). A 0.526 cm^2 punch of a quartz filter sample was heated in a stepwise manner to obtain data for three elemental carbon (EC) fractions. At the same time, OP (pyrolyzed carbon) was produced at $< 580^{\circ}\text{C}$ in the inert atmosphere, which decreases the reflected light to correct for charred OC. Total EC is the sum of the three EC fractions minus OP. More details and QA/QC (quality assurance and quality control) are shown by Cao et al. (2003, 2009).

The rBC (refractory black carbon), which is used instead of BC for measurements derived from incandescence methods (Petzold et al., 2013), was analyzed at the Institute of Tibetan Plateau Research, Chinese Academy of Sciences, by using a Single Particle Soot Photometer (SP2) coupled with an ultrasonic nebulization system (CETAC UT5000). The mass of the rBC of individual particles was measured by using laser-induced incandescence (Schwarz et al., 2006). The incandescence signal can be converted to rBC mass which is detected by photomultiplier tube detectors. Previous studies have successfully applied this analytical method to ice core research (McConnell et al., 2007; Kaspari et al., 2011; Biseau et al., 2012). Detailed descriptions of the SP2 analytical process and calibration procedures can be found in Wendl et al. (2014) and Wang et al. (2015b).

Although there are differences in the two analytical techniques (Wang et al., 2015b), in order to facilitate the discussions, they are uniformly referred to as black carbon (BC) in our study since both of them share some of the characteristics of BC with its light-absorbing properties (Petzold et al., 2013).

2.4 Global chemistry transport model/MOZART-4

The model used in this study is MOZART-4 (Model for Ozone and Related chemical Tracers, version 4). The model is an offline global chemical transport model for the troposphere developed jointly by the National Center for Atmospheric Research (NCAR), the Geophysical Fluid Dynamics Laboratory (GFDL), and the Max Planck Institute for Meteorology (MPI-Met). The detailed model description and model evaluated can be found in Emmons et al. (2010). The aerosol modules were developed by Tie et al. (2005). This model has been developed and used to quantify the global budget of trace gases and aerosol particles, and to study their atmospheric transport, chemical transformations and removal (Emmons et al., 2010; Chang et al., 2016). The model is built based on the framework of the Model of Atmospheric Transport and Chemistry (MATCH) (Rasch et al., 1997). Convective mass fluxes are diagnosed by using the shallow and mid-level convective transport formulation of Hack (1994) and the deep convection scheme (Zhang and McFarlane, 1995). Vertical diffusion within the boundary layer is built on the parameterization by Holtslag and Boville (1993). An advective transport scheme used the flux form semi-Lagrangian transport algorithm (Lin and Rood, 1996). The wet deposition includes in-cloud as well as below-cloud scavenging developed by Brasseur et al. (1998) and is taken into MOZART-4. Details of the chemical solver scheme can be found in the Auxiliary Material by Kinnison et al. (2007).

In the present study, the model includes 85 gas-phase species, 12 bulk aerosol compounds and approximately 200 reactions. The horizontal resolution of this study is $1.9^\circ \times 2.5^\circ$ with 56 hybrid sigma-pressure vertical levels from the surface to approximately 2 hPa. The meteorological initial and boundary conditions are downloaded from the NCAR Community Data Portal (CDP), using National Centers for Environmental Prediction (NCEP) meteorology. The model transport of this study is driven by the Modern-Era Retrospective-analysis for Research and Applications (MERRA) 6-hour reanalysis data with a $1.9^\circ \times 2.5^\circ$ grid provided by the National Aeronautics and Space Administration (NASA).

The BC emission inventory used in this global model is based on the simulation of the POET (Precursors of Ozone and their Effects in the Troposphere) database from 1997 to 2007 and the data of the BC emission inventory including fossil fuel and biofuel combustion from a previous study (Bond et al., 2004). Figure 2 illustrates the updated 21-year average global BC emissions from 1986 to 2006. There are two types of black carbon particles in MOZART-4, hydrophobic and hydrophilic particles. Hydrophobic particles are directly emitted from the sources, and are converted to hydrophilic particles in the atmosphere (Hagen et al., 1992; Lioussé et al., 1993; Parungo et al., 1994), with a rate constant of $7.1 \times 10^{-6} \text{ s}^{-1}$ (Cooke and Wilson, 1996).

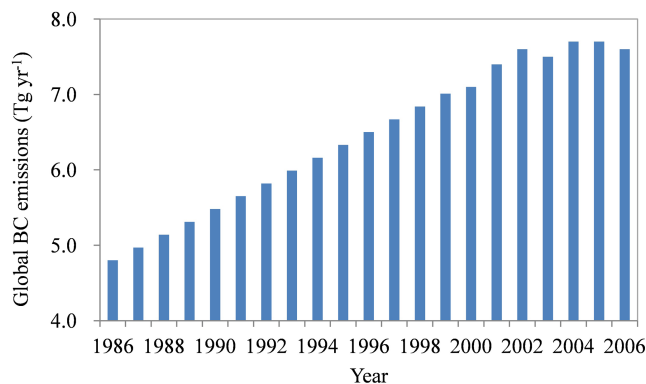


Figure 2. The trend of global BC emission (Tg yr^{-1}) from 1986 to 2006 used in this study.

2.5 BC deposition estimation

In order to compare it to the measured ice core BC deposition at Muztagh Ata Mountain, the BC deposition flux is calculated in this study. In the estimation, the calculated atmospheric BC concentrations and precipitation data obtained from the China Meteorological Data Service Center were compiled and evaluated. In addition, annual BC deposition parameters and deposition flux calculation methods were described in other studies (Jurado et al., 2008; Yasunari et al., 2010; Fang et al., 2015; Li et al., 2017). In brief, deposition fluxes are calculated by the following equations:

$$F_{\text{DD}} = 10^{-4} v_{\text{D}} C_{\text{BC}} t, \quad (1)$$

$$F_{\text{WD}} = 10^{-7} p_0 W_{\text{p}} C_{\text{BC}}, \quad (2)$$

$$F_{\text{BC}} = F_{\text{DD}} + F_{\text{WD}}, \quad (3)$$

where 10^{-4} and 10^{-7} are unit conversion factors; F_{DD} and F_{WD} are the annual dry and wet deposition (ng cm^{-2}), respectively; the total BC deposition flux (F_{BC}) (ng cm^{-2}) is the sum of F_{DD} and F_{WD} , where v_{D} (m s^{-1}) is the dry deposition velocity of black carbon; t is total estimation time for 1 year (s); p_0 is the annual precipitation rate (mm); W_{p} is the particle washout ratio (dimensionless); and C_{BC} is the annual atmospheric BC concentrations at Muztagh Ata Mountain (ng m^{-3}). There are large differences in estimates on v_{D} and W_{p} (Jurado et al., 2005, 2008; Yasunari et al., 2013). A fixed small dry deposition velocity of $1.0 \times 10^{-4} \text{ m s}^{-1}$ onto snow was adopted (Yasunari et al., 2010; Nair et al., 2013) and the corresponding estimation values are likely to represent a lower bound for BC dry deposition in this area. Particle washout ratio W_{p} is assumed to be a constant and equal to 2×10^5 , which has been adopted in many modeling exercises and fits well with field measurements (Mackay et al., 1986; Jurado et al., 2005; Fang et al., 2015; Li et al., 2017).

3 Results and discussion

3.1 Model evaluation and compared to observation

In order to better understand the variation, characteristics, and source contributions of the BC concentrations at Muztagh Ata Mountain, model-sensitive studies using MOZART-4 were conducted in this study. Firstly, the model was evaluated by comparing the observed monthly BC concentrations with the calculated monthly BC concentrations during January 2004 to February 2006. As shown in Fig. 3a, the simulated BC concentrations had a similar magnitude of measured BC concentrations, with mean values of 62.4 and 56.5 ng m^{-3} for the calculation and measurement, respectively. It was also evident that the measured variability of BC was captured by the calculation. For example, the calculated variability was comparable to the measured result between July 2014 and October 2015. However, some differences were also noticeable. For example, the calculated BC concentration was overestimated in the spring and winter of 2004 and underestimated in the winter of 2006. Because the measured site is located in a “clean” region of BC emission, the BC particles were mostly transported from a long distance of the upwind regions. There were uncertainties related to the emissions and simulated meteorological parameters (wind speeds, wind directions, etc.). As a result, it caused the discrepancy between calculated and measured BC concentrations at Muztagh Ata Mountain. There was another reason that may cause the difficulty of the calculation. The horizontal resolution of the global model is relatively low ($1.9^\circ \times 2.5^\circ$ in this study), which is unable to reproduce some detailed variability in the simulation. However, the overall features of the measured BC concentrations were reproduced by the model, such as the magnitude and seasonal variability (see Fig. 3b), suggesting that the model is capable of studying long-range transport from BC source regions to the remote site.

The simulated seasonal variation is shown in Fig. 3b. The result shows that calculated seasonal variation generally agreed with the measured variation, except for the value in spring. According to the analysis of the source contribution (shown in Sect. 3.3), the BC emission in South Asia has significant contributions to the BC concentrations at Muztagh Ata during the non-summer season which accounted for an average of 31%–60% in spring and few contributions in the summer season. The overestimated BC concentrations may due to the fact that the model overestimated the pollutant transportation from the emission sources to the sampling site crossing the high mountains of the Tibetan Plateau, which act as a wall to block the transportation from the BC emission in South Asia to the sampling area (Zhao et al., 2013).

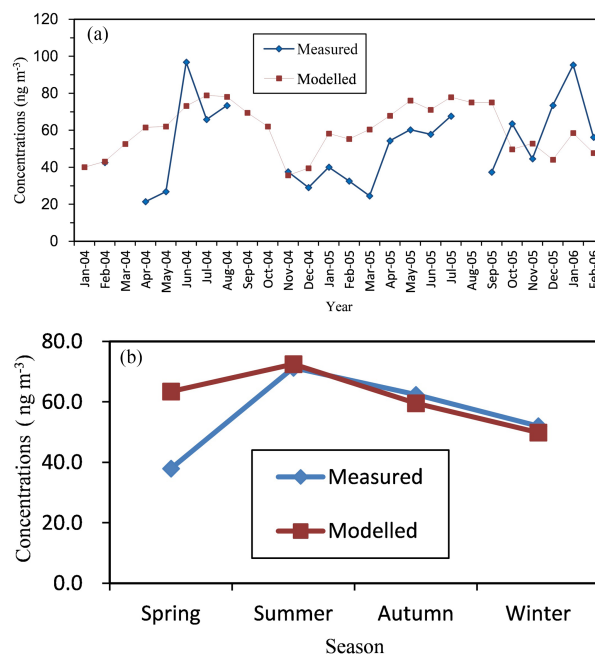


Figure 3. (a) Comparison of calculated (red) and measured (blue) monthly mean BC concentrations at the surface level during January 2004 to February 2006 measured by the Cold and Arid Regions Environmental and Engineering Institute, Chinese Academy of Sciences. (b) Comparison of calculated (red) and measured (blue) seasonal variations during January 2004 to February 2006. Spring includes March, April and May in 2004 and 2005. Summer includes June, July and August in 2004 and 2005; autumn includes September, October and November in 2004 and 2005; winter includes December, January and February of 2004 and 2005 and January and February in 2006.

3.2 Long-term ice core measurement and possible effects of the Kuwait fire event

In addition to the atmospheric sampling of BC measurement, there is a long-term ice core measurement of BC at Muztagh Ata Mountain. This long-term measurement represents valuable data to show the long-term trend and inter-annual variability. Ice core records obtained at Muztagh Ata Mountain are invaluable when evaluating contemporary atmospheric or snow BC concentration variations. A long-term ice-core measurement (from 1940 to 2010) was provided by Xu et al. (2009a) at Muztagh Ata Mountain. Their results showed that the ice core BC concentrations were between 0.30 and 39.54 ng g^{-1} from 1940 to 2010, with an average value of 7.22 ng g^{-1} . The BC deposition fluxes were between 9.96 and 909.88 ng cm^{-2} , with an average of 184.18 ng cm^{-2} . It is interesting to note that both BC concentration and BC deposition of ice cores showed a sharp increase in 1992, which was about 5 times higher than the average mean value as shown in Fig. 4. No other similar peak was found in the entire

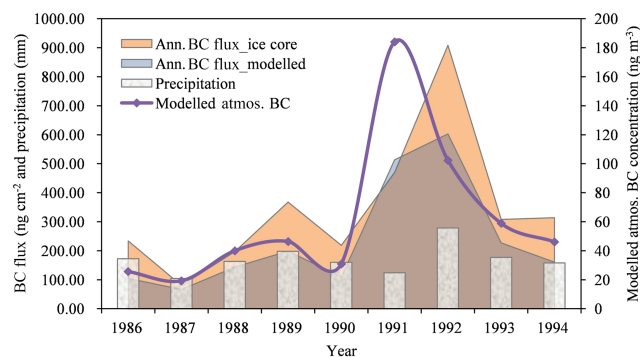


Figure 4. Comparison of measured annual BC deposition flux with the model calculation between ice core and simulation, as well as the modeled atmospheric BC concentration and precipitation used for BC deposition flux calculation.

record, which may indicate a specific event that led to this sharp increase, which provides useful information to track the BC emissions. In this study, we conduct several model studies to investigate this special event.

As shown in Fig. 4, there was a high BC deposition flux (900 ng cm^{-2}) in 1992, compared to $100\text{--}300 \text{ ng cm}^{-2}$ in other years. In order to investigate this special event, we focus our model study on a short period (from 1986 to 1994). One potential reason to cause this sharp increase in BC was that during 1991, when Iraqi troops withdrew from Kuwait at the end of the first Gulf War, they set a huge fire to over 700 oil wells. The fires were started in January and February 1991, and the last well was capped on 6 November 1991. The resulting fires produced a large plume of smoke and particles that had significant effects on the Persian Gulf area and the potential for global effects (as shown in Fig. 5).

In order to estimate the intensity of the BC emission from the fires, Hobbs and Radke (1992) conducted two aircraft studies during the period 16 May through 12 June 1991 to evaluate the effects of the smoke. The estimated emission rate of elemental carbon of the Kuwait fires is ~ 3400 metric tons day^{-1} , which is 13 times the BC emissions from all U.S. combustion sources in total.

In order to study the effect of the huge Kuwait fires on the BC ice core deposition, the MOZART-4 model was applied to simulate the atmospheric BC concentrations and deposition flux variation from 1986 to 1994. Several model sensitivity studies were conducted. First, the atmospheric BC concentration was calculated by the anthropogenic BC emission with the default emissions (POET) as described before. Second, in order to simulate the large increase in the BC emissions caused by the Kuwait fires in the Persian Gulf (Region 3 in Fig. 1), according to the measured values of Hobbs and Radke (1992), the BC emissions were significantly enhanced by 50 times from January to November 1991 to represent Kuwait fires. Figure 4 shows the horizontal distribu-

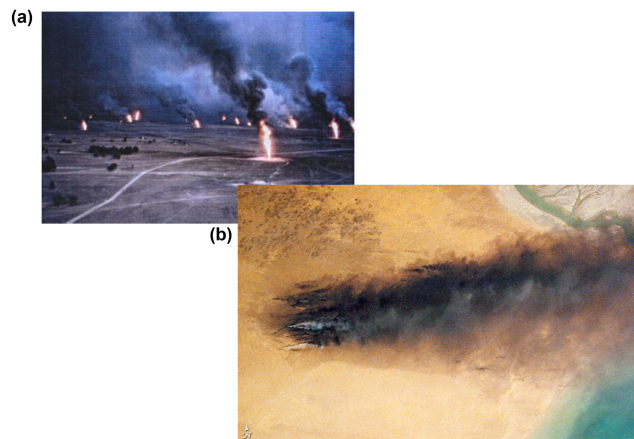


Figure 5. The image of the fires in Kuwait during 1991. It shows the intensive fires and the rise of plumes due to the heat buoyancy. The lower panel shows the fires were transported east due to winds from the west.

tion of the calculated BC plume from the Kuwait fires, with the enhanced BC emission.

The calculated result suggests that there was a significant increase in BC concentrations nearby the Kuwait fires (see Fig. 6). The BC concentrations reached $10\text{--}20 \mu\text{g m}^{-3}$ at the surface (see Fig. 6a) and more than $0.7 \mu\text{g m}^{-3}$ at 5 km above the surface (see Fig. 6b). As shown in Figs. 5 and 6, the winds nearby the fire region were in the northern and northwestern directions. Because the lifetime of black carbon aerosols is sufficiently long (about a week) (Ramanathan et al., 2001; Bauer et al., 2013), the high BC concentrations were transported westwards toward Muztagh Ata Mountain.

The evaluation of the modeled BC deposition at Muztagh Ata Mountain was conducted by comparison between the calculation and measurement (see Fig. 4). Figure 4 shows the calculated temporal variation of BC concentrations and deposition, which were compared with the measured variations. The result shows that the calculated temporal variability of BC deposition was generally consistent with the measured variability. For example, both high peaks of calculated and measured BC deposition occurred in 1992. The calculated atmospheric concentrations of BC, however, had a peak value in 1991. This was due to the fact that the deposition of BC in ice cores was an accumulated value, while the atmospheric BC concentration was an in situ value. Despite the consistency of temporal variations between measured and calculated deposition of BC, there was a consistent underestimation of calculated BC deposition compared to the measured value. Because there were uncertainties in estimates of BC emission and the deposition, these uncertainties could result in the discrepancy between the calculation and measurement. For example, according to the assimilation meteorological data by the Chinese Meteorological Administration, the annual precipitation in 1992 was about twice as high as

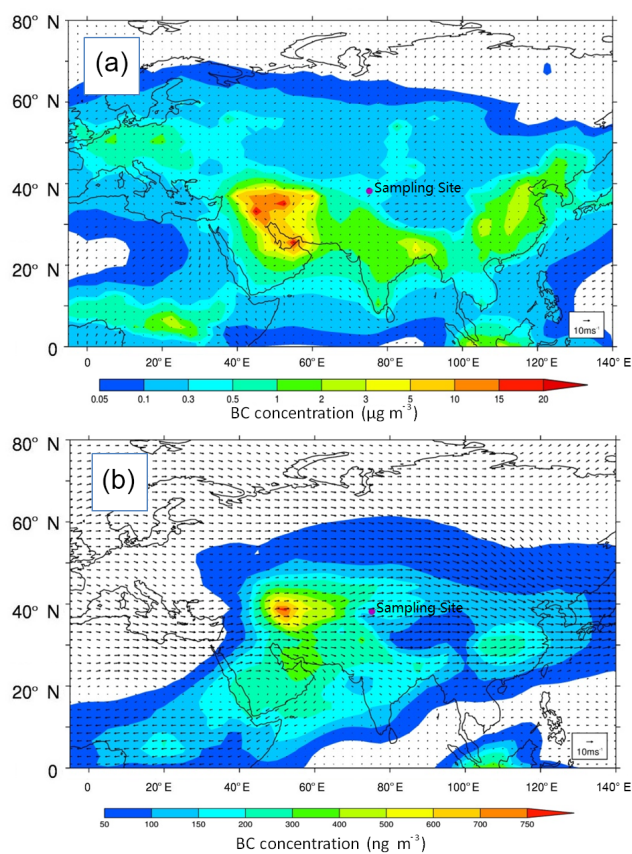


Figure 6. The calculated horizontal distributions of BC concentrations ($\mu\text{g m}^{-3}$) at the surface (a) and the concentrations (ng m^{-3}) at 5 km above the surface (b) in Kuwait during 1991. The wind direction and speed are indicated by black arrows.

in 1991 at the nearby Muztagh Ata Mountain, suggesting that scavenging efficiency may likely be underestimated, causing the calculated uncertainty in the estimate of the BC deposition.

3.3 Effect of regional BC emissions at Muztagh Ata Mountain

To further understand the influence of transportation and deposition on the annual variation of BC at Muztagh Ata Mountain (as a receptor region), sensitivity experiments using the MOZART-4 model were conducted. In the sensitivity study, the effect of different BC emission regions on the BC concentrations at the measurement site was individually calculated. Four primary regions were defined with latitude and longitude as shown in Table 1 and Fig. 1, including (R1) Central Asia, (R2) Europe, (R3) the Persian Gulf, and (R4) South Asia. Central Asia, Europe and South Asia previously have been reported as significant BC emission sources of Muztagh Ata Mountain (Liu et al., 2008; Xu et al., 2009a; Wang et al., 2015b). Europe is one of the biggest emission sources of the world, located in the upwind region of the receptor site

although it is far away. Central Asia and South Asia are surrounding emission sources of the receptor site. The Persian Gulf could be a potential emission source which could have been overlooked before. In each sensitivity study, only the individual BC emission was included, and the BC emissions in other regions were excluded. As a result, the fractional contributions by the individual emission regions to BC concentrations in the receptor region (Muztagh Ata Mountain) were calculated. Table 1 shows the calculated results.

In order to clearly show the transport pathways from the different regions to the measurement site and the Tibetan Plateau, the calculated horizontal distributions of BC concentrations from each region during three different periods (summer monsoon, non-monsoon, and annual mean) are shown in Fig. 7.

The results from Table 1 and Fig. 7 suggest that during the “normal period” (non-Kuwait fires), the BC emissions from Central Asia and South Asia had the largest contributions to the BC concentrations at the measurement site, contributing annual means of 27 % and 25 %, respectively. It is interesting to note that there were strong seasonal variations regarding the effects. During the monsoon period, the largest effect was due to the Central Asia source (44 %), while during the non-monsoon period, the largest effect was due to the South Asia source (34 %).

As shown in Fig. 7, during the monsoon period, the airflow from the oceans (Persian Gulf and Bay of Bengal) moves northward and is coupled with the strong precipitation. As a result, the BC particles from South Asian sources were washed out during the transport pathway, leading to lower BC concentrations at the measurement site. In contrast, during the non-monsoon period, the prevailing winds were western winds, and BC emission in northern India was transported to the measurement site, leading to higher BC concentrations. The contributions from Persian Gulf emissions to the BC concentrations were generally low. However, during the Kuwait fires period, this region had a significant contribution to the Muztagh Ata area as well as the Tibetan Plateau.

3.4 Radiative forcing induced by BC in the Muztagh Ata glacier

The deposition of BC on the snow reduces the surface albedo, causing a positive radiative forcing and increases in ice melt and snowmelt. Previous studies show that BC particles produce significant reduction in the snow albedo with the solar visible wavelengths (Warren and Wiscombe, 1980). In this study, the effect of BC deposition on the snow albedo and radiative forcing during 1986 to 1994 in the Muztagh Ata glacier was estimated. The SNICAR online model (Snow, Ice, and Aerosol Radiation; available at <http://snow.engin.umich.edu>, last access: 28 December 2017) (Flanner and Zender, 2005; Flanner et al., 2007) was used to estimate the effect of BC particles on snow albedo at different solar wavelengths.

Table 1. Source regions and corresponding fractional contributions to atmospheric BC concentrations at the Muztagh Ata site in monsoon, non-monsoon and all months during 1993. NA – not available.

	Source regions	Latitude	Longitude	Summer monsoon (June–September)	Non-monsoon (October–May)	Annual
R1	Central Asia	37–56° N	50–95° E	43.9 %	18.1 %	26.7 %
R2	Europe	35–67° N	0–50° E	26.6 %	11.5 %	16.5 %
R3	Persian Gulf	24–35° N	35–55° E	9.4 %	12.1 %	11.2 %
R4	South Asia	14–37° N	55–95° E	7.3 %	33.7 %	24.9 %
	Others	NA	NA	7.9 %	6.2 %	6.8 %

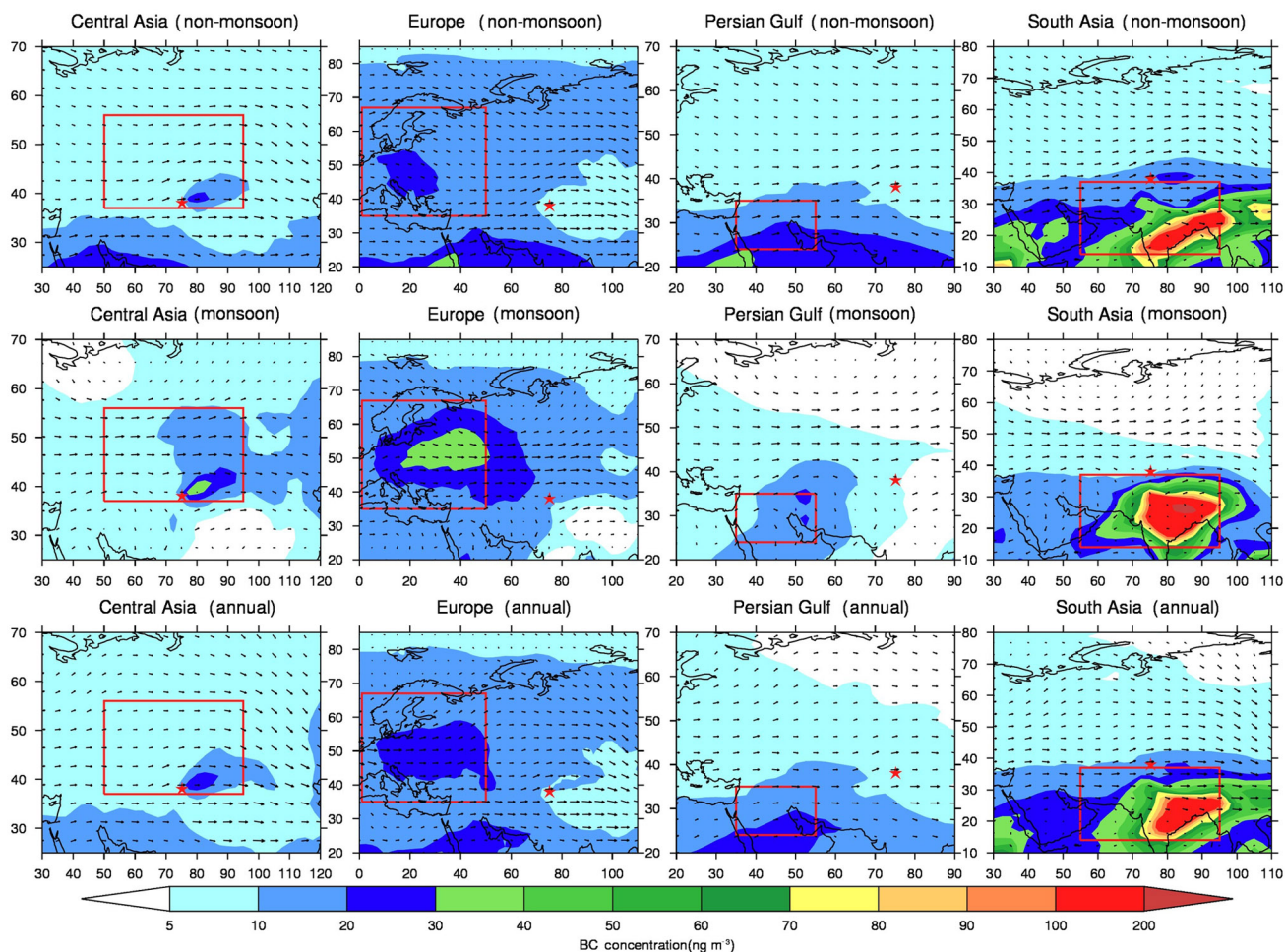


Figure 7. The calculated spatial BC distributions due to individual BC from the four source regions (Central Asia, Europe, Persian Gulf and South Asia) above 5 km above the surface during different periods, i.e., monsoon (June–September), non-monsoon (October–May), and annual mean in 1993. The red star is where the study site of Muztagh Ata located. The red boxes indicate the boundary of the four source regions.

To estimate the effect of the BC deposition on surface albedo, in addition to the BC concentrations, there are several environmental factors such as snow grain size, solar zenith angle, and snow depth that need to be estimated (Warren and Wiscombe, 1980). The setup of input parameters required for

running the SNICAR model is briefly described as below. As we focus on the calculation of radiative forcing caused by BC particles, other impurity contents, such as dust and volcanic ash, were set to zero. A mass absorption cross section (MAC) of $7.5 \text{ m}^2 \text{ g}^{-1}$ at 550 nm for uncoated BC par-

ticles (Bond and Bergstrom, 2006) was assumed to be the same as the default value, and the MAC scaling factor in the online SNICAR model as one of the input parameters was set to 1.0. The effective radius of $100\ \mu\text{m}$ with a density of $60\ \text{kg m}^{-3}$ was used for new snow, and the effective radius of $400\ \mu\text{m}$ with a density of $400\ \text{kg m}^{-3}$ was adopted for the albedo estimation according to the previous studies and measurements in other studies on the Tibetan Plateau (Wiscombe and Warren, 1980; Wu et al., 2006). The extractive snow height from MERRA (the Modern-Era Retrospective-analysis for Research and Applications) reanalysis products was used for snowpack thickness. The forcing dataset used in this study was developed by the Data Assimilation and Modeling Center for Tibetan Multi-spheres, Institute of Tibetan Plateau Research, Chinese Academy of Sciences (Chen et al., 2011). The recovered BC concentrations of ice cores were used as the input parameter of uncoated black carbon concentration. The averaged short-wave flux and solar zenith angle of each month were obtained from the China Meteorological Forcing Dataset provided by the Data Assimilation and Modeling Center for Tibetan Multi-spheres, Institute of Tibetan Plateau Research, Chinese Academy of Sciences.

The measured average BC concentration in the ice core during 1986–1994 was $15.2\ \text{ng g}^{-1}$, with a peak value of $39.2\ \text{ng g}^{-1}$. The calculated snow albedo reduction by using the SNICAR model ranged from 0.11 % to 1.36 % by assuming that the snow layer was totally covered by fresh snow (lower limit). However, if it was an aged layer, the estimated snow albedo reduction increased, ranging from 0.47 % to 2.97 % (upper limit). The actual value should lie between the two ranges. This result is consistent with the previous studies. For example, Yasunari et al. (2010) reported that the reduction of snow albedo ranged from 2.0 % to 5.2 %, with a BC concentration of $26.0\text{--}68.2\ \text{ng g}^{-1}$, based on atmospheric BC measurements at NCO-P over the southern slopes of the western Himalayas.

The reduction of snow albedo enhanced the absorption of solar energy and accelerated snowmelt and ice melt (Conway et al., 1996). Several studies suggested that BC containments on snow were very effective at reducing the surface albedo (Warren and Wiscombe, 1980; Petr Chylek and Srivastava, 1983; Gardner and Sharp, 2010). In this study, the effects of BC containments on snow albedo and snow water equivalent (SWE) reduction were estimated.

Figure 8 shows the calculated effects of BC containments on annual mean radiative forcing increase (RFI) (W m^{-2}) and snow water equivalent (SWE) reduction (mm yr^{-1} ; millimeters per year), under fresh snow assumption and aged snow assumption. The results show that under the fresh snow assumption (lower limit), the increases in RFI ranged from 0.2 to $2.5\ \text{W m}^{-2}$, while under the aged snow assumption (upper limit), the increases in RFI ranged from 0.9 to $5.7\ \text{W m}^{-2}$. This estimate is consistent with the previous studies (Flanner et al., 2009). During the Kuwait fires pe-

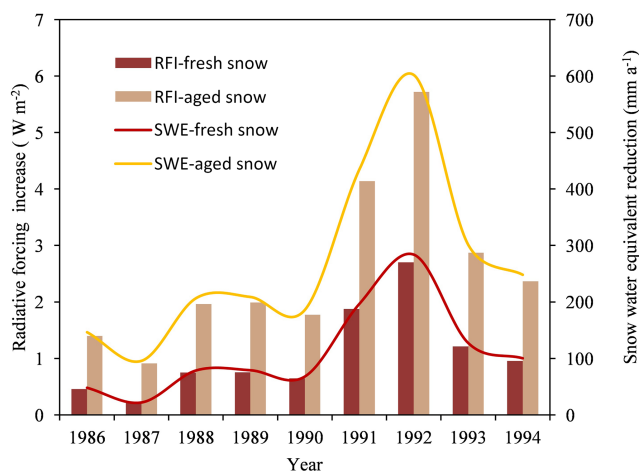


Figure 8. Estimated effects of BC containments on annual mean radiative forcing increase (RFI) (W m^{-2}) and snow water equivalent (SWE) reduction (mm yr^{-1}), under fresh snow assumption (purple line and bars) and aged snow assumption (yellow line and bars).

riod, the RFI values increased about 2–5 times, which led to a significant increase for the snow melting during the period.

The potential influence for BC deposition on glaciers from forest fires that was highlighted was coincident with an increase in discharge downriver in the previous study (Kaspari et al., 2015). The runoff of the melted snow due to the increase in snow surface albedo was estimated in this study. A first-order estimation was based on the additional energy contribution to the snowpack due to BC deposition. First the melting point of snow was estimated. Second, the extra snowmelt from light-absorbing black carbon was estimated by dividing hourly instantaneous radiative forcing by the enthalpy of fusion of water at $0\ ^\circ\text{C}$ of $0.334 \times 10^6\ \text{J kg}^{-1}$ (Painter et al., 2013; Kaspari et al., 2015). The estimation represented the snowmelt in kg m^{-2} across the hour during acquisition, or melt in millimeters snow water equivalent (SWE). The melted snow due to the BC water was calculated (shown in Fig. 8). The result shows that the estimated averaged SWE reductions were 111 and 270 mm, for fresh and aged snow, respectively. During the Kuwait fires period, the estimated SWE significantly increased, reaching 600 mm for aged snow condition and 300 mm for fresh snow condition. The increase was about 3 times that of pre- and post-Kuwait fires, suggesting that this special event had a significant impact on snow melting for the Tibetan glaciers and the water resources in the region. However, this estimate of runoff is speculative since there are a number of influential factors. Schmale et al. (2017) found that the combination effect of meteorological parameters and snow albedo could be 3 times larger than model results. The Tibetan Plateau is recognized as the “Water Tower of Asia”, with a large contribution to the annual river discharge of the Yangtze River, Indus, Brahmaputra, etc. The snowmelt runoff will impact on the regional

climate system, including the timing of runoff and the frequency and intensity of floods and rainfall patterns because of its tightening interaction with the hydrologic cycle (Jain et al., 2010). Wu and Qian (2003) reported that Tibetan winter snow cover is abnormally linked to rainfall over South, Southeast and East Asia by observation data analysis.

4 Conclusions

Black carbon (BC) particles change the radiative balance of the atmosphere by absorbing and scattering solar radiation. As a result, BC deposition on the surface of snow and ice changes the albedo of solar radiation. Albedo change is the key parameter to affect the melting of glaciers on the Tibetan Plateau. In order to study this effect, two sets of measurements were used to study the variability of BC deposition at Muztagh Ata Mountain, northern Tibetan Plateau. The measured data included the air samplings of BC particles during 2004–2006 and the ice core drillings of BC deposition during 1986–1994. To identify the effect of BC emissions on the BC deposition in this region, a global chemical transportation model (MOZART-4) was used to analyze the BC transport from the source regions. A radiative transfer model (SNICAR) was used to study the effect of BC deposition on snow albedo.

The results show some important highlights to reveal the temporal variability of BC deposition and the effect of long-range transport on the BC pollution in the northern Tibetan Plateau, which are summarized as follows.

1. During 1991–1992, there was a strong spike in the BC deposition at Muztagh Ata, suggesting that there was an unusual emission in the upward region. This high peak in BC deposition was investigated by using the global chemical transportation model (MOZART-4). The analysis indicated that the emissions from large Kuwait fires at the end of the first Gulf War in 1991 caused the high peak in the BC concentrations and the BC deposition. As a result, the BC deposition in 1991 and 1992 at Muztagh Ata Mountain was 3–4 times higher than other periods.
2. The effect of Kuwait fires on the BC deposition at Muztagh Ata Mountain suggested that the upward BC emissions had important impacts on this remote site located on the northern Tibetan Plateau. In order to quantitatively estimate the effect of surrounding emissions on the BC concentrations on the northern Tibetan Plateau, a sensitive study with four individual BC emission regions (Central Asia, Europe, the Persian Gulf, and South Asia) was conducted by using the MOZART-4 model. The result suggests that during the “normal period” (non-Kuwait fires), the largest effect was due to the Central Asia source (44 %) during the Indian

monsoon period. During the non-monsoon period, the largest effect was due to the South Asia source (34 %).

3. The increase in radiative forcing increase (RFI) due to the deposition of BC on snow was estimated by using the radiative transfer model (SNICAR). The results show that under the fresh snow assumption, the estimated RFI ranged from 0.2 to 2.5 W m⁻², while under the aged snow assumption, the estimated RFI ranged from 0.9 to 5.7 W m⁻². During the Kuwait fires period, the RFI values increased about 2–5 times higher than the “normal period”, suggesting a significant increase for the snow melting on the northern Tibetan Plateau due to this fire event.

This result suggests that the variability of BC deposition at Muztagh Ata Mountain provides useful information to study the effect of the upward BC emissions on environmental and climate issues in the northern Tibetan Plateau. The radiative effect of BC deposition on the snow melting provides important information regarding the water resources in the region.

Data availability. Measurement data for air and ice core samples and other datasets needed to reproduce the results shown in this paper can be obtained on request (via Xuexi Tie, tiexx@ieecas.cn) from the owners.

Author contributions. JZ carried out the research. XT, BX, and JZ designed the research. JZ, XT, SZ, GL, and LC developed and evaluated the MZ4 model. SY, ZZ, and MW provided radiation data and model output. BX, MW, and SY provided ice core data. SL, TZ, ZZ, and JC provided air particle data. JZ, XT, GL, SZ, LC, and MW wrote the text.

Competing interests. The authors declare that they have no conflict of interest.

Acknowledgements. This work was supported by the National Natural Science Foundation of China (NSFC) under grant nos. 41430424, 41730108 and 41230641. The authors thank the Center for Excellence in Urban Atmospheric Environment, Institute of Urban Environment, Chinese Academy of Sciences, for their support. The National Center for Atmospheric Research is sponsored by the National Science Foundation.

Edited by: Jianping Huang

Reviewed by: two anonymous referees

References

An, Z. S., Kutzbach, J. E., Prell, W. L., and Porter, S. C.: Evolution of Asian monsoons and phased uplift of the Himalaya-

- Tibetan plateau since Late Miocene times, *Nature*, 411, 62–66, <https://doi.org/10.1038/35075035>, 2001.
- Bauer, S. E., Bausch, A., Nazarenko, L., Tsigaridis, K., Xu, B., Edwards, R., Bisiaux, M., and McConnell, J.: Historical and future black carbon deposition on the three ice caps: Ice core measurements and model simulations from 1850 to 2100, *J. Geophys. Res.-Atmos.*, 118, 7948–7961, <https://doi.org/10.1002/jgrd.50612>, 2013.
- Bisiaux, M. M., Edwards, R., McConnell, J. R., Curran, M. A. J., Van Ommen, T. D., Smith, A. M., Neumann, T. A., Pasteris, D. R., Penner, J. E., and Taylor, K.: Changes in black carbon deposition to Antarctica from two high-resolution ice core records, 1850–2000 AD, *Atmos. Chem. Phys.*, 12, 4107–4115, <https://doi.org/10.5194/acp-12-4107-2012>, 2012.
- Bond, T. C. and Bergstrom, R. W.: Light Absorption by Carbonaceous Particles: An Investigative Review, *Aerosol Sci. Tech.*, 40, 27–67, <https://doi.org/10.1080/02786820500421521>, 2006.
- Bond, T. C., Streets, D. G., Yarber, K. F., Nelson, S. M., Woo, J.-H., and Klimont, Z.: A technology-based global inventory of black and organic carbon emissions from combustion, *J. Geophys. Res.*, 109, 1042, <https://doi.org/10.1029/2003JD003697>, 2004.
- Brasseur, G. P., Hauglustaine, D. A., Walters, S., Rasch, P. J., Müller, J.-F., Granier, C., and Tie, X. X.: MOZART, a global chemical transport model for ozone and related chemical tracers: 1. Model description, *J. Geophys. Res.*, 103, 28265–28289, <https://doi.org/10.1029/98JD02397>, 1998.
- Cao, J. J., Lee, S. C., Ho, K. F., Zhang, X. Y., Zou, S. C., Fung, K., Chow, J. C., and Watson, J. G.: Characteristics of carbonaceous aerosol in Pearl River Delta Region, China during 2001 winter period, *Atmos. Environ.*, 37, 1451–1460, [https://doi.org/10.1016/S1352-2310\(02\)01002-6](https://doi.org/10.1016/S1352-2310(02)01002-6), 2003.
- Cao, J. J., Xu, B. Q., He, J. Q., Liu, X. Q., Han, Y. M., Wang, G. H., and Zhu, C. S.: Concentrations, seasonal variations, and transport of carbonaceous aerosols at a remote Mountainous region in western China, *Atmos. Environ.*, 43, 4444–4452, 2009.
- Chang, L. Y., Xu, J. M., Tie, X. X., and Wu, J. B.: Impact of the 2015 El Nino event on winter air quality in China, *Sci. Rep.*, 6, 34275, <https://doi.org/10.1038/srep34275>, 2016.
- Chen, Y., Yang, K., He, J., Qin, J., Shi, J., Du, J., and He, Q.: Improving land surface temperature modeling for dry land of China, *J. Geophys. Res.*, 116, D20104, <https://doi.org/10.1029/2011JD015921>, 2011.
- Chow, J. C., Watson, J. G., Pritchett, L. C., Pierson, W. R., Frazier, C. A., and Purcell, R. G.: The dri thermal/optical reflectance carbon analysis system: Description, evaluation and applications in U.S. Air quality studies, *Atmos. Environ. A-Gen.*, 27, 1185–1201, [https://doi.org/10.1016/0960-1686\(93\)90245-T](https://doi.org/10.1016/0960-1686(93)90245-T), 1993.
- Chow, J. C., Watson, J. G., Chen, L. W. A., Arnott, W. P., Moosmüller, H., and Fung, K.: Equivalence of elemental carbon by thermal/optical reflectance and transmittance with different temperature protocols, *Environ. Sci. Technol.*, 38, 4414–4422, 2004.
- Conway, H., Gades, A., and Raymond, C. F.: Albedo of dirty snow during conditions of melt, *Water Resour. Res.*, 32, 1713–1718, <https://doi.org/10.1029/96WR00712>, 1996.
- Cooke, W. F. and Wilson, J. J. N.: A global black carbon aerosol model, *J. Geophys. Res.*, 101, 19395–19409, <https://doi.org/10.1029/96JD00671>, 1996.
- Emmons, L. K., Walters, S., Hess, P. G., Lamarque, J.-F., Pfister, G. G., Fillmore, D., Granier, C., Guenther, A., Kinnison, D., Laepple, T., Orlando, J., Tie, X., Tyndall, G., Wiedinmyer, C., Baughcum, S. L., and Kloster, S.: Description and evaluation of the Model for Ozone and Related chemical Tracers, version 4 (MOZART-4), *Geosci. Model Dev.*, 3, 43–67, <https://doi.org/10.5194/gmd-3-43-2010>, 2010.
- Fang, Y., Chen, Y. J., Tian, C. G., Lin, T., Hu, L. M., Huang, G. P., Tang, J. H., Li, J., and Zhang, G.: Flux and budget of BC in the continental shelf seas adjacent to Chinese high BC emission source regions, *Global Biogeochem. Cy.*, 29, 957–972, <https://doi.org/10.1002/2014GB004985>, 2015.
- Flanner, M. G. and Zender, C. S.: Snowpack radiative heating: Influence on Tibetan Plateau climate, *Geophys. Res. Lett.*, 32, L06501, <https://doi.org/10.1029/2004GL022076>, 2005.
- Flanner, M. G., Zender, C. S., Randerson, J. T., and Rasch, P. J.: Present-day climate forcing and response from black carbon in snow, *J. Geophys. Res.*, 112, 3131, <https://doi.org/10.1029/2006JD008003>, 2007.
- Flanner, M. G., Zender, C. S., Hess, P. G., Mahowald, N. M., Painter, T. H., Ramanathan, V., and Rasch, P. J.: Springtime warming and reduced snow cover from carbonaceous particles, *Atmos. Chem. Phys.*, 9, 2481–2497, <https://doi.org/10.5194/acp-9-2481-2009>, 2009.
- Gardner, A. S. and Sharp, M. J.: A review of snow and ice albedo and the development of a new physically based broadband albedo parameterization, *J. Geophys. Res.*, 115, D13203, <https://doi.org/10.1029/2009JF001444>, 2010.
- Hack, J. J.: Parameterization of moist convection in the National Center for Atmospheric Research community climate model (CCM2), *J. Geophys. Res.*, 99, 5551, <https://doi.org/10.1029/93JD03478>, 1994.
- Hagen, D. E., Trueblood, M. B., and Whitefield, P. D.: A Field Sampling of Jet Exhaust Aerosols, *Particul. Sci. Technol.*, 10, 53–63, <https://doi.org/10.1080/02726359208906598>, 1992.
- Hansen, J. and Nazarenko, L.: Soot climate forcing via snow and ice albedos, *P. Natl. Acad. Sci. USA*, 101, 423–428, 2004.
- Hobbs, P. V. and Radke, L. F.: Airborne studies of the smoke from the kuwait oil fires, *Science*, 256, 987–991, <https://doi.org/10.1126/science.256.5059.987>, 1992.
- Holben, B. N., Eck, T. F., Slutsker, I., Tanré, D., Buis, J. P., Setzer, A., Vermote, E., Reagan, J. A., Kaufman, Y. J., Nakajima, T., Lavenu, F., Jankowiak, I., and Smirnov, A.: AERONET – A Federated Instrument Network and Data Archive for Aerosol Characterization, *Remote Sens. Environ.*, 66, 1–16, [https://doi.org/10.1016/S0034-4257\(98\)00031-5](https://doi.org/10.1016/S0034-4257(98)00031-5), 1998.
- Holtlag, A. A. M. and Boville, B. A.: Local Versus Nonlocal Boundary-Layer Diffusion in a Global Climate Model, *J. Climate*, 6, 1825–1842, 1993.
- Jain, S. K., Goswami, A., and Saraf, A. K.: Assessment of Snowmelt Runoff Using Remote Sensing and Effect of Climate Change on Runoff, *Water Resour. Manag.*, 24, 1763–1777, <https://doi.org/10.1007/s11269-009-9523-1>, 2010.
- Jurado, E., Jaward, F., Lohmann, R., Jones, K. C., Simó, R., and Dachs, J.: Wet Deposition of Persistent Organic Pollutants to the Global Oceans, *Environ. Sci. Technol.*, 39, 2426–2435, <https://doi.org/10.1021/es048599g>, 2005.
- Jurado, E., Dachs, J., Duarte, C. M., and Simó, R.: Atmospheric deposition of organic and black carbon to

- the global oceans, *Atmos. Environ.*, 42, 7931–7939, <https://doi.org/10.1016/j.atmosenv.2008.07.029>, 2008.
- Kaspari, S., McKenzie Skiles, S., Delaney, I., Dixon, D., and Painter, T. H.: Accelerated glacier melt on Snow Dome, Mount Olympus, Washington, USA, due to deposition of black carbon and mineral dust from wildfire, *J. Geophys. Res.-Atmos.*, 120, 2793–2807, <https://doi.org/10.1002/2014JD022676>, 2015.
- Kaspari, S. D., Schwikowski, M., Gysel, M., Flanner, M. G., Kang, S., Hou, S., and Mayewski, P. A.: Recent increase in black carbon concentrations from a Mt. Everest ice core spanning 1860–2000 AD, *Geophys. Res. Lett.*, 38, 155–170, <https://doi.org/10.1029/2010GL046096>, 2011.
- Kinnison, D. E., Brasseur, G. P., Walters, S., Garcia, R. R., Marsh, D. R., Sassi, F., Harvey, V. L., Randall, C. E., Emmons, L., Lamarque, J. F., Hess, P., Orlando, J. J., Tie, X. X., Randel, W., Pan, L. L., Guttman, A., Granier, C., Diehl, T., Niemeier, U., and Simmons, A. J.: Sensitivity of chemical tracers to meteorological parameters in the MOZART-3 chemical transport model, *J. Geophys. Res.*, 112, 32295, <https://doi.org/10.1029/2006JD007879>, 2007.
- Lavanchy, V. M. H., Gäggeler, H. W., Schotterer, U., Schwikowski, M., and Baltensperger, U.: Historical record of carbonaceous particle concentrations from a European high-alpine glacier (Colle Gnifetti, Switzerland), *J. Aerosol Sci.*, 30, S611–S612, [https://doi.org/10.1016/S0021-8502\(99\)80316-4](https://doi.org/10.1016/S0021-8502(99)80316-4), 1999.
- Li, C., Yan, F., Kang, S., Chen, P., Han, X., Hu, Z., Zhang, G., Hong, Y., Gao, S., Qu, B., Zhu, Z., Li, J., Chen, B., and Silanpää, M.: Re-evaluating black carbon in the Himalayas and the Tibetan Plateau: concentrations and deposition, *Atmos. Chem. Phys.*, 17, 11899–11912, <https://doi.org/10.5194/acp-17-11899-2017>, 2017.
- Lin, S.-J. and Rood, R. B.: Multidimensional Flux-Form Semi-Lagrangian Transport Schemes, *Mon. Weather Rev.*, 124, 2046–2070, 1996.
- Lioussé, C., Cachier, H., and Jennings, S. G.: Optical and thermal measurements of black carbon aerosol content in different environments: Variation of the specific attenuation cross-section, σ (σ), *Atmos. Environ. A-Gen.*, 27, 1203–1211, [https://doi.org/10.1016/0960-1686\(93\)90246-U](https://doi.org/10.1016/0960-1686(93)90246-U), 1993.
- Liu, X. Q., Xu, B. Q., Yao, T. D., Wang, N. L., and Wu, G. J.: Carbonaceous particles in Muztagh Ata ice core, West Kunlun Mountains, China, *Sci. Bull.*, 53, 3379–3386, <https://doi.org/10.1007/s11434-008-0294-5>, 2008.
- Mackay, D., Paterson, S., and Schroeder, W. H.: Model describing the rates of transfer processes of organic chemicals between atmosphere and water, *Environ. Sci. Technol.*, 20, 810–816, <https://doi.org/10.1021/es00150a009>, 1986.
- McConnell, J. R., Edwards, R., Kok, G. L., Flanner, M. G., Zender, C. S., Saltzman, E. S., Banta, J. R., Pasteris, D. R., Carter, M. M., and Kahl, J. D. W.: 20th-century industrial black carbon emissions altered Arctic climate forcing, *Science*, 317, 1381–1384, <https://doi.org/10.1126/science.1144856>, 2007.
- Ming, J., Cachier, H., Xiao, C., Qin, D., Kang, S., Hou, S., and Xu, J.: Black carbon record based on a shallow Himalayan ice core and its climatic implications, *Atmos. Chem. Phys.*, 8, 1343–1352, <https://doi.org/10.5194/acp-8-1343-2008>, 2008.
- Nair, V. S., Babu, S. S., Moorthy, K. K., Sharma, A. K., Marinoni, A., and Ajai: Black carbon aerosols over the Himalayas: Direct and surface albedo forcing, *Tellus B*, 65, 19738, <https://doi.org/10.3402/tellusb.v65i0.19738>, 2013.
- Painter, T. H., Seidel, F. C., Bryant, A. C., McKenzie Skiles, S., and Rittger, K.: Imaging spectroscopy of albedo and radiative forcing by light-absorbing impurities in mountain snow, *J. Geophys. Res.-Atmos.*, 118, 9511–9523, <https://doi.org/10.1002/jgrd.50520>, 2013.
- Parungo, F., Nagamoto, C., Zhou, M.-Y., Hansen, A. D. A., and Harris, J.: Aeolian transport of aerosol black carbon from Aeolian transport of aerosol black carbon from China to the ocean, *Atmos. Environ.*, 28, 3251–3260, 1994.
- Petr Chylek, V. R. and Srivastava, V.: Albedo of soot-contaminated snow, *J. Geophys. Res.*, 88, 10837–10843, 1983.
- Petzold, A., Ogren, J. A., Fiebig, M., Laj, P., Li, S.-M., Baltensperger, U., Holzer-Popp, T., Kinne, S., Pappalardo, G., Sugimoto, N., Wehrli, C., Wiedensohler, A., and Zhang, X.-Y.: Recommendations for reporting “black carbon” measurements, *Atmos. Chem. Phys.*, 13, 8365–8379, <https://doi.org/10.5194/acp-13-8365-2013>, 2013.
- Ramanathan, V., Crutzen, P. J., Kiehl, J. T., and Rosenfeld, D.: Aerosols, climate, and the hydrological cycle, *Science*, 294, 2119–2124, 2001.
- Rasch, P. J., Mahowald, N. M., and Eaton, B. E.: Representations of transport, convection, and the hydrologic cycle in chemical transport models: Implications for the modeling of short-lived and soluble species, *J. Geophys. Res.*, 102, 28127–28138, 1997.
- Schmale, J., Flanner, M., Kang, S., Sprenger, M., Zhang, Q., Guo, J., Li, Y., Schwikowski, M., and Farinotti, D.: Modulation of snow reflectance and snowmelt from Central Asian glaciers by anthropogenic black carbon, *Sci. Rep.*, 7, 40501, <https://doi.org/10.1038/srep40501>, 2017.
- Schwarz, J. P., Gao, R. S., Fahey, D. W., Thomson, D. S., Watts, L. A., Wilson, J. C., Reeves, J. M., Darbeheshti, M., Baumgardner, D. G., Kok, G. L., Chung, S. H., Schulz, M., Hendricks, J., Lauer, A., Kärcher, B., Slowik, J. G., Rosenlof, K. H., Thompson, T. L., Langford, A. O., Loewenstein, M., and Aikin, K. C.: Single-particle measurements of midlatitude black carbon and light-scattering aerosols from the boundary layer to the lower stratosphere, *J. Geophys. Res.*, 111, 2845, <https://doi.org/10.1029/2006JD007076>, 2006.
- Tie, X. X., Madronich, S., Walters, S., Edwards, D. P., Ginoux, P., Mahowald, N., Zhang, R. Y., Lou, C., and Brasseur, G.: Assessment of the global impact of aerosols on tropospheric oxidants, *J. Geophys. Res.*, 110, D03204, <https://doi.org/10.1029/2004JD005359>, 2005.
- Wang, M., Xu, B., Cao, J., Tie, X., Wang, H., Zhang, R., Qian, Y., Rasch, P. J., Zhao, S., Wu, G., Zhao, H., Joswiak, D. R., Li, J., and Xie, Y.: Carbonaceous aerosols recorded in a southeastern Tibetan glacier: analysis of temporal variations and model estimates of sources and radiative forcing, *Atmos. Chem. Phys.*, 15, 1191–1204, <https://doi.org/10.5194/acp-15-1191-2015>, 2015a.
- Wang, M., Xu, B. Q., Kaspari, S. D., Gleixner, G., Schwab, V. F., Zhao, H. B., Wang, H. L., and Yao, P.: Century-long record of black carbon in an ice core from the Eastern Pamirs: Estimated contributions from biomass burning, *Atmos. Environ.*, 115, 79–88, <https://doi.org/10.1016/j.atmosenv.2015.05.034>, 2015b.
- Warren, S. G. and Wiscombe, W. J.: A Model for the Spectral Albedo of Snow. II: Snow Containing Atmospheric Aerosols, *J. Atmos. Sci.*, 37, 2734–2745, 1980.

- Wendl, I. A., Menking, J. A., Färber, R., Gysel, M., Kaspari, S. D., Laborde, M. J. G., and Schwikowski, M.: Optimized method for black carbon analysis in ice and snow using the Single Particle Soot Photometer, *Atmos. Meas. Tech.*, 7, 2667–2681, <https://doi.org/10.5194/amt-7-2667-2014>, 2014.
- Wiscombe, W. J. and Warren, S. G.: A Model for the Spectral Albedo of Snow. I: Pure Snow, *J. Atmos. Sci.*, 37, 2712–2733, 1980.
- Wu, G. J., Yao, T. D., Xu, B. Q., Li, Z., Tian, L. D., Duan, K. Q., and Wen, L. K.: Grain size record of microparticles in the Muztagata ice core, *Sci. China Ser. D*, 49, 10–17, <https://doi.org/10.1007/s11430-004-5093-5>, 2006.
- Wu, G. J., Yao, T. D., Xu, B. Q., Tian, L. D., Li, Z., and Duan, K. Q.: Seasonal variations of dust record in the Muztagata ice cores, *Sci. Bull.*, 53, 2506–2512, <https://doi.org/10.1007/s11434-008-0197-5>, 2008.
- Wu, T. and Qian, Z.: The relation between the Tibetan winter snow and the Asian summer monsoon and rainfall: an observational investigation, *J. Climate*, 16, 2038–2051, 2003.
- Xu, B., Cao, J., Hansen, J., Yao, T., Joswita, D. R., Wang, N., Wu, G., Wang, M., Zhao, H., Yang, W., Liu, X., and He, J.: Black soot and the survival of Tibetan glaciers, *P. Natl. Acad. Sci. USA*, 106, 22114–22118, <https://doi.org/10.1073/pnas.0910444106>, 2009a.
- Xu, B. Q., Wang, M., Joswiak, D. R., Cao, J. J., Yao, T. D., Wu, G. J., Yang, W., and Zhao, H. B.: Deposition of anthropogenic aerosols in a southeastern Tibetan glacier, *J. Geophys. Res.*, 114, 9185, <https://doi.org/10.1029/2008JD011510>, 2009b.
- Yasunari, T. J., Bonasoni, P., Laj, P., Fujita, K., Vuillermoz, E., Marinoni, A., Cristofanelli, P., Duchi, R., Tartari, G., and Lau, K.-M.: Estimated impact of black carbon deposition during pre-monsoon season from Nepal Climate Observatory – Pyramid data and snow albedo changes over Himalayan glaciers, *Atmos. Chem. Phys.*, 10, 6603–6615, <https://doi.org/10.5194/acp-10-6603-2010>, 2010.
- Yasunari, T. J., Tan, Q., Lau, K.-M., Bonasoni, P., Marinoni, A., Laj, P., Ménégoz, M., Takemura, T., and Chin, M.: Estimated range of black carbon dry deposition and the related snow albedo reduction over Himalayan glaciers during dry pre-monsoon periods, *Atmos. Environ.*, 78, 259–267, <https://doi.org/10.1016/j.atmosenv.2012.03.031>, 2013.
- Zhang, G. J. and McFarlane, N. A.: Sensitivity of climate simulations to the parameterization of cumulus convection in the Canadian climate centre general circulation model, *Atmos. Ocean*, 33, 407–446, <https://doi.org/10.1080/07055900.1995.9649539>, 1995.
- Zhao, H. B., Xu, B. Q., Yao, T. D., Tian, L. D., and Li, Z.: Records of sulfate and nitrate in an ice core from Mount Muztagata, central Asia, *J. Geophys. Res.*, 116, D13304, <https://doi.org/10.1029/2011JD015735>, 2011.
- Zhao, Z., Cao, J., Shen, Z., Xu, B., Zhu, C., Chen, L.-W. A., Su, X., Liu, S., Han, Y., Wang, G., and Ho, K.: Aerosol particles at a high-altitude site on the Southeast Tibetan Plateau, China: Implications for pollution transport from South Asia, *J. Geophys. Res.-Atmos.*, 118, 11360–11375, <https://doi.org/10.1002/jgrd.50599>, 2013.